

THE DYNAMICS OF MAGNETORHEOLOGICAL ELASTOMERS STUDIED BY SYNCHROTRON RADIATION SPECKLE ANALYSIS

W. F. SCHLOTTER, C. CIONCA, S. S. PARUCHURI, J. B. CUNNINGHAM,
E. DUFRESNE, S.B. DIERKER, D. ARMS, AND R. CLARKE
University of Michigan, Ann Arbor, MI 48109-1120 USA
E-mail: wschlott@umich.edu

J. M. GINDER AND M. E. NICHOLS
Ford Motor Company, Research Laboratory, Dearborn, MI 48121-2053 USA

We introduce a new technique for probing the microscopic relaxation of magneto-viscoelastic materials consisting of magnetic particles embedded in a natural rubber matrix. Transversely coherent x-rays from a high brilliance synchrotron source are scattered by the magnetic particles, forming a speckle pattern at low scattering angles. The time dependence of this pattern is recorded with a CCD area detector while the sample is cyclically perturbed by a reversal of the magnetic field direction. The corresponding time-resolved scattering pattern probes both the dynamics of the particles and the relaxation of the matrix in which they are embedded. X-ray photon correlation spectroscopy (XPCS) reveals characteristic time scales for this relaxation by applying the intensity auto-correlation function to the time dependent speckle pattern. For low angle scattering, the wave vector dependence of the relaxation rate exhibits power law length scaling.

1 Introduction

Magnetic particles embedded in a polymer matrix enable myriad applications such as data storage media, heat activated printing toner and flexible permanent magnets. When these particles are embedded in a cross-linked elastomer the composite material displays an increase in dynamic stiffness when introduced to an applied magnetic field.¹ Such composites are known as magnetorheological (MR) elastomers or magneto-viscoelastic materials and are the solid state analog of MR fluids.² During cross-linking or curing, each particle in an MR elastomer is locked in position until magnetic or mechanical perturbations induce particle configurations of lower energy. Following such a disturbance each particle will approach its original energy state as the elastomer relaxes. Weakly interacting embedded particles will yield to the path dictated by the matrix material. This suggests a method for measuring the relaxation dynamics of any matrix on a microscopic level.³

Photon correlation spectroscopy (PCS) has previously been employed to measure particle dynamics in ER and MR fluids.^{4,5} The wavelength of visible light limits such studies to minimum length scales of a few hundred

nanometers. Moreover, the optical properties of ferromagnetic particulates and the natural rubber matrix make MR elastomers opaque to visible light; however, high intensity x-ray synchrotron radiation can penetrate bulk samples thereby providing a microscopic probe of the composite structure and its dynamics.

X-ray photon correlation spectroscopy (XPCS) was recently employed to measure the diffusive behavior of gold colloids and binary fluids.⁶ When coherent x-ray wave fronts are scattered at the particle-host interface, they produce a speckle interference pattern.⁷ The time dependence of this intensity pattern can be correlated to explore the characteristic times associated with the motion of scatterers in the sample. We have extended the use of this technique to MR elastomer samples at the Advanced Photon Source, Argonne National Laboratory. This third generation x-ray synchrotron source accelerates relativistic electrons through arrays of permanent magnets known as undulators, thus producing extremely intense quasi-monochromatic x-ray radiation. Excellent transverse and longitudinal coherence of the beam enables interfering wave fronts at the scattering interface to produce a speckle interference pattern.

2 Experimental Method

2.1 MR Elastomer Samples

Magnetite particles (Magneox Pulaski, TMB-X-1539) with an average size of ~200nm were embedded in a natural rubber, cis-polyisoprene, matrix with a $\phi \approx 0.25$ particulate volume fraction. Samples with an average thickness of 100 μm were mounted on a glass slide and cured at 140°C in the absence of an applied magnetic field.

2.2 Small Angle Scattering Setup

Monochromatic x-rays were used to probe the sample as shown in the configuration in Figure 1. The transverse coherence of the beam is ~10 μm in the vertical direction and ~4 μm in the horizontal. Coherence (S_1) and guard slits (S_2) are used to select only the transversely coherent section of the beam. Both of these square apertures accept a 100 μm^2 beam cross section. For this geometry and x-ray wavelength, the size of a single speckle spot was calculated to be 8 μm . The coherent beam enters a hole in the first pole piece of the dipole electromagnet, GMW-3470, and travels

18 cm to the sample (MR_1). The sample was rigidly mounted in a 6 mm gap between the pole pieces and the direction of the applied magnetic field was reversed periodically. Tapered axial holes were bored in each pole piece, allowing the beam to travel parallel to the field lines in the sample.

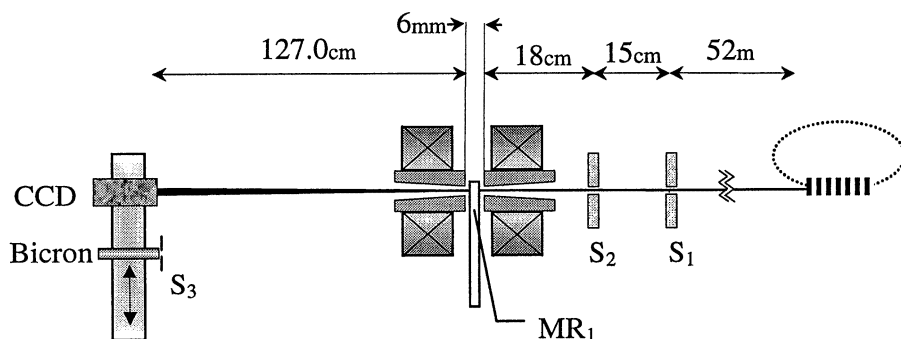


Figure 1: Schematic arrangement for small-angle XPCS measurements. X-rays from the undulator source at right are scattered from the MR elastomer sample in transmission geometry. Slits are used to isolate the coherent section of the beam for scattering. Time dependent scattering is recorded with a CCD area detector or a Bicron photo multiplier point detector mounted on a translating stage.

2.3 CCD detector

Time dependent speckle patterns were measured with a CCD chip positioned to capture directly the small-angle scattering. The sample-detector distance shown in Fig. 1 is chosen so that the speckle size is a good match to the CCD pixel resolution. A Bicron photomultiplier detector with $64 \mu\text{m}^2$ slits (S_3) was used for calibration, but the CCD was selected for data acquisition due to the following attributes:

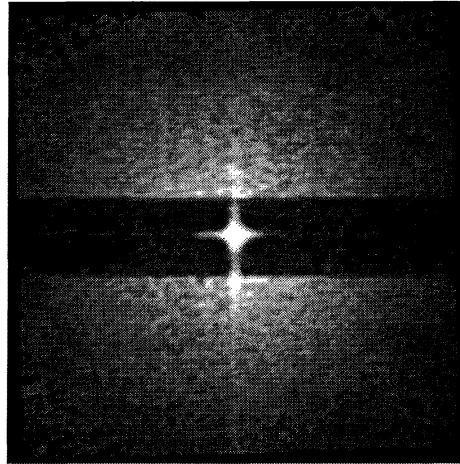
- Efficient parallel data acquisition
- Ability to access very small scattering angles, corresponding to small scattering wave vectors, $0.001 \text{ \AA}^{-1} < q < 0.01 \text{ \AA}^{-1}$
- Enhanced statistics enabled by averaging over annular regions of fixed q

A Texas Instruments TC253 low noise, high sensitivity CCD with $7.4 \mu\text{m}$ pixel width in a 658×494 array was controlled by a 12-bit QMAX 650 camera.⁸ Digital images were transmitted to a microcomputer and recorded as a movie with KSA 400 image acquisition software.⁹ 100-frame movies were recorded at 0.42 Hz with a 1.8 second exposure duration.

3 Experimental Results

We first consider the static small-angle intensity profile, which is generated by averaging the intensity of each pixel in every frame of a scattering movie with respect to time. The resulting two dimensional matrix can be represented as the time averaged image shown in Fig. 2. The main beam is observed in the middle of the rectangular shadow of the beam stop and shows weak Fraunhofer diffraction features characteristic of a square aperture. This is a signature of the coherent light necessary for speckle interference. A profile of radial intensity with respect to wave vector was extracted from the data of Fig. 2 and fit to a Guinier curve.¹⁰ This predicts the particle size to be $300 \pm 100 \text{ nm}$, consistent with SEM micrographs and product literature.

Figure 2: Integrated scattering intensity pattern. The image is 200 pixels on a side and subtends 1.1 mrad. Note the weak Fraunhofer diffraction feature for a square aperture. The horizontal area of low intensity dividing the circular pattern is the shadow of the beam stop. By summing the intensity of each pixel at a constant angle the average intensity at a specific wave vector was determined. These plots were then used to determine the average particle size in the Guinier approximation



4 Analysis

4.1 Intensity correlation

Temporal fluctuations in intensity were recorded for each pixel and characterized with the intensity auto-correlation function,¹¹

$$g_2(\Delta t) = \frac{\langle I(t + \Delta t)I(t) \rangle}{\langle I(t) \rangle^2},$$

where $I(t)$ is the intensity at a time t and all averages are over time. Correlation results for each pixel were averaged with others of similar wavevector magnitude, q where $q = (4\pi/\lambda)\sin\theta$. The time dependence of these data reflects the scatter motion at specific wave vectors, Fig. 3.

Fitting these data to exponential decay curves, also plotted in Fig. 3, quantifies the characteristic time constants. For weakly interacting particles this relaxation is characteristic of the matrix material.

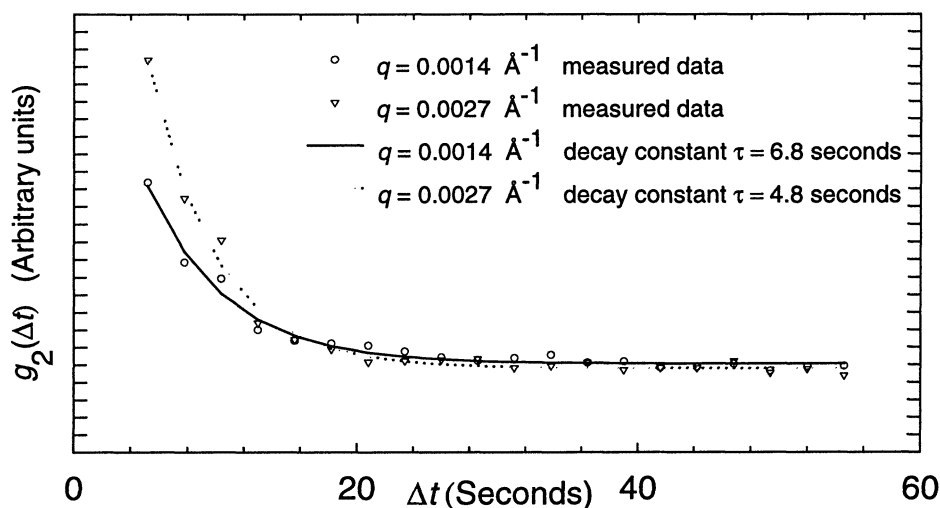


Figure 3: Plot of the azimuthally averaged auto-correlation results for $q = 0.0014 \text{ \AA}^{-1}$ and $q = 0.0027 \text{ \AA}^{-1}$ with corresponding exponential relaxation curves.

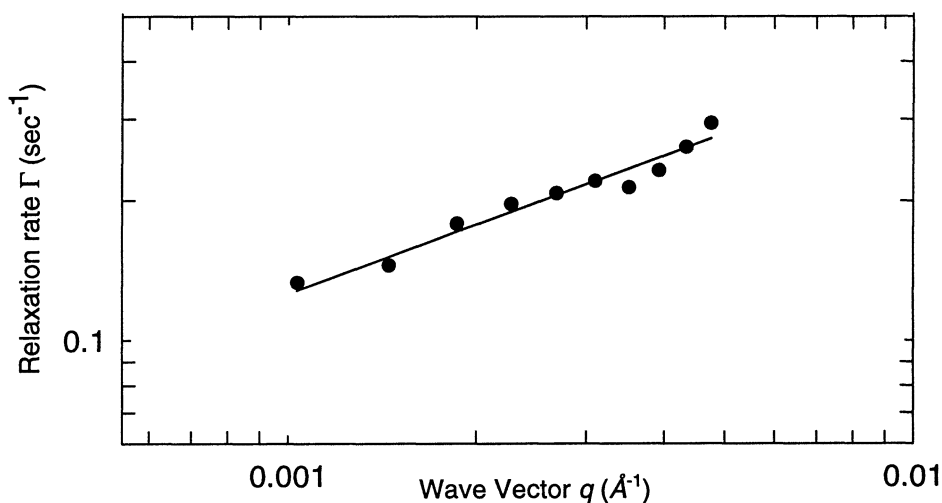


Figure 4: Scaling of the relaxation rate with scattering wave vector. The solid line is a fit to $q^{0.49}$.

4.2 Wave vector dependence of time decay

A characteristic relaxation rate, Γ , for the material is found by taking the inverse of the time constant. The relaxation rate is found to vary as a power law in q , the magnitude of the scattering wave vector, as shown in Fig. 4.

5 Discussion

Qualitatively similar power law dependence is observed in other scattering systems. For example, colloidal media undergoing Brownian motion show a q^2 relaxation rate dependence.¹² While thermal excitations may contribute to the dynamics of our elastomer samples, the changing magnetic field provides the dominant source of excitation for the particles. In contrast to the behavior of diffusive systems, where the relaxation rate scales like q^2 , we observed $\sim q^{0.5}$. Whether this represents true power law scaling, or a crossover to q independent behavior at small q remains to be checked with more detailed studies.

From the data, the relaxation rate for a macroscopic wave vector $q = 0$ can be approximated to be around 0.02 Hz. This limiting rate is consistent with the effects of macroscopic mechanical perturbation of the material, which relax on time scales on the order of one minute. This quasi-static behavior is expected in the viscoelastic terminal region of cross-linked polymers.¹³ In this region viscoelastic losses dominate the elastic restoration force resulting in an overdamped system.

6 Conclusions

Clearly, these results show that XPCS is a practical technique for measuring the dynamic behavior of particles embedded in viscoelastic materials. The use of high intensity x-ray synchrotron radiation and CCD area detectors allows for real-time measurements on visibly opaque media. Intensity auto-correlation functions were calculated from time dependent speckle patterns, which were recorded as movies. Exponential time decays were fit to these correlations at specific wave vectors. The inverse of the decay time, the relaxation rate Γ , has a power law relationship to wave vector. Unlike the quadratic q dependence characteristic of diffusive media, sub-linear behavior is observed in this case. We are in the process of formulating a quantitative model for this observed behavior. One preliminary conclusion is that algebraic scaling of the kind we observed is

indicative of dynamics governed by affine processes. (i.e. self similar structure which relaxes without selecting a particular length scale) Through a better understanding of particle dynamics in weakly interacting systems this technique serves as a novel probe of the viscoelastic properties of MR materials.

Acknowledgment

The authors would like to thank Larry Elie and Teamour Nurushev. Use of the Advanced Photon Source was supported by the U.S. Department of Energy, Office of Science, Office of Basic Energy Sciences, under Contract No. W-31-109-ENG-38. The experiments were conducted at MHATT-CAT Sector 7, which is supported by Department of Energy Grant DE-FG02-99ER45743.

References

- ¹ J.M. Ginder, M. E. Nichols, L. D. Elie, and J. L. Tardiff, "Magnetorheological Elastomers: Properties and Applications", *Smart Structures and Materials 1999: Smart Material Technologies*, ed. by M. Wuttig, (1999) pp. 131-138.
- ² J.M. Ginder, "Rheology Controlled by Magnetic Fields", *Encyclopedia of Applied Physics*, VCH Publishers, Inc., **16**, (1996) pp. 487-503.
- ³ P.D. Kaplan, V. Trappe, and D.A. Weitz, "Light-scattering microscope," *Applied Optics*, **38**, (1999) pp. 4151-57.
- ⁴ M. Hagenbüchle, P. Sheaffer, Y. Zhu and J. Liu, "Static and Dynamic Light Scattering of Dilute MR Emulsions," *Proceedings of the 5th International Conference on ERM*, ed. by W. Bullough, World Scientific, (1996) pp. 236-239.
- ⁵ J.M. Ginder, "Diffuse optical probes of particle motion and structure formation in an electrorheological fluid", *Phys. Rev. E*, **47**, (1993) pp. 3418-3447.
- ⁶ S.B. Dierker, R. Pindak, R.M. Fleming, I.K. Robinson, L. Berman, "X-Ray Photon Correlation Spectroscopy Study of Brownian Motion of Gold Colloids in Glycerol", *Phys. Rev. Lett.* **75**, (1995) pp. 449-452.
- ⁷ M. Sutton, S.G.J. Mochrie, T. Greytak, S.E. Magler, L.E. Berman, G.A. Held, G.B. Stephenson, "Observation of speckle by diffraction with coherent X-rays", *Nature* **352**, (1991) pp. 608-610.
- ⁸ CCD Direct, Ann Arbor, MI.
- ⁹ k-Space Associates Inc. Ann Arbor, MI.
- ¹⁰ O. Glatter, O. Kratky, *Small Angle X-ray Scattering*, Academic Press, (1982) p. 155.
- ¹¹ see B. Chu, *Laser Light Scattering*, Academic Press, (1994) p. 94.
- ¹² T. Nurushev, *Studies of Static and Dynamic Critical Behavior of Simple Binary Fluids and Polymer Mixtures using XPCS*, PhD Thesis, University of Michigan, (2000).
- ¹³ J.D. Ferry, *Viscoelastic Properties of Polymers*, Wiley, (1970).